Int. J. Nonlinear Anal. Appl. In Press, 1–10
ISSN: 2008-6822 (electronic)
http://dx.doi.org/10.22075/ijnaa.2024.35531.5286

Seismic behavior analyses of reinforced tunnel with steel fiber reinforced concrete (SFRC) composites by consideration of optimum thickness in artificial neural network (ANN) analyses

Hootan Fakharian[a], Hadi Bahadori[b,*], Mohamadali Ramezanpour[a], Ali Dehghanbanadaki[c]

[a]*Department of Civil Engineering, Rudehen Branch, Islamic Azad University, Rudehen, Iran*

[b]*Department of Civil Engineering, Urmia University, Urmia, Iran*

[c]*Department of Civil Engineering, Damavand Branch, Islamic Azad University, Damavand, Iran*

(Communicated by Majid Eshaghi Gordji)

Abstract

This study is organized in two parts. In the first part, the seismic behaviour of tunnels reinforced with steel fibre-reinforced concrete composites (SFRC) fibre reinforcing is investigated and using the finite element method (FEM) in ABAQUS software, 3 different models of the thickness (similar in terms of compressive strength and tensile strength) have been evaluated in the Tehran Metro tunnel. In this section, to apply seismic force, the PGA characteristics of the El Centro earthquake in the United States have been used, and the parameters of force and displacement concerning time have been extracted. In the second part, using the effect of three different thicknesses of 20, 40 and 60 cm in determining the behaviour of the tunnel under the earthquake, the amount of stress and displacement over time was extracted. These results were investigated using two models of neural networks, MLP and RBF, to determine the optimal thickness to withstand stress and displacement in the tunnel. It was also found that the optimal thickness of the tunnel was obtained using MLP and RBF networks to control stress of 47.95 cm and 48.22 cm, respectively, and to control displacement of 47.21 cm and 48.15 cm, respectively. Finally, it can be acknowledged that using the optimal thicknesses, the maximum stress tolerance by MLP and RBF methods is equal to $1.7556 \times 10^{+6}$ N/m^2 and $1.9289 \times 10^{+6}$ N/m^2 is obtained. Also, the highest amount of displacement with both methods (due to the good accuracy of both models in determining the displacement) is equal to 0.0256 cm.

Keywords: seismic analyses, reinforced tunnel, thickness, neural network
2020 MSC: 68T07

1 Introduction

This tunnel is one of the largest long-distance tunnels. Given that the tunnel area is prone to earthquake activity, the seismic performance of the tunnel is investigated for the 120-year design life of the structure. Furthermore, due to the spatial variation of earthquake motions along tunnels [18, 5, 10]. The influence of non-uniform seismic

*Corresponding author
Email addresses: hootanfakharian@gmail.com (Hootan Fakharian), h.bahadori@urmia.ac.ir (Hadi Bahadori), ma.ramezanpour@riau.ac.ir (Mohamadali Ramezanpour), deghanbanadaki@damavandiau.ac.ir (Ali Dehghanbanadaki)

Received: August 2024 *Accepted:* November 2024

excitations on the tunnel needs to be evaluated and considered for its seismic design [20, 19]. Tunnels constitute a major part of civil infrastructure and serve as public transportation facilities, sanitation, irrigation utilities and storage infrastructure [18]. In seismically active areas, these tunnels are at earthquake-induced risk. Recent events such as the Kobe Earthquake in Japan, the Duzce Earthquake in Turkey, the Chi-Chi Earthquake in Taiwan, the Bam Earthquake in Iran and the Wenchuan Earthquake in China have shown that tunnels are susceptible to irrecoverable damage due to seismic loading [18, 17], some quite extensively [16]. The observed damage provides sufficient evidence to suggest that the safety of tunnels in seismically active areas is still an important issue, but not well understood yet or at least not well considered during design. Shear deformation of tunnels induced by the vertically propagating shear waves has been widely studied by several researchers [3, 6, 1], and it has been known to be the critical mode of deformation for tunnels under seismic loading. The tunnel lining is generally simulated as a buried structure subjected to ground deformations under a two-dimensional plane strain condition. Two basic approaches are commonly used to estimate the response of tunnels under shear deformation. One approach is to carry out dynamic, nonlinear soil-structure interaction analysis using finite element methods. The input motions in these analyses are time histories emulating design response spectra, and the input motions are applied to the boundaries of a "soil island" to represent vertically propagating shear waves. The second approach assumes that the seismic ground motions induce a pseudo-static loading condition to the structure. This approach allows the development of analytical relationships to evaluate the magnitude of seismically induced strains in the tunnel structure [12, 11, 4].

These relationships are based on the premise that tunnel structures under seismic loading will tend to deform due to the demand from surrounding ground, and thus the structure is designed to accommodate the imposed deformations without loss of its structural integrity. Xiong et al. [15] employed numerical simulation and model tests to investigate the mechanical response and damage mechanism of the stick-slip dislocation on the fault. Russo et al. [13] relied on the Bolu Tunnel and the Kohhrangs Tunnel, respectively, and used numerical simulation methods to carry out a comparative study on the effect of reducing dislocation joints with different pitch-span ratios on the secondary lining. Liu et al. [8], Liu and Gao [9], and Wang et al. [14] used the model test to study the anti-breaking effect of the measures of reducing dislocation joints, reducing dislocation layers, and thickening the secondary lining. Using the method of theoretical analysis and model test, Wang et al. [14] and Liu et al. [7] studied the damping model, damping mechanism, fault, and parameter sensitivity of the damping layer. Avanaki et al. [2] analysed the effects of different steel fibre-reinforced concrete (SFRC) composites on the flexural response of segmental joints under seismic actions and investigated them numerically based on experimental results. The results in terms of moment-rotation (M–h) curves derived from an experimental test setup are used to calibrate and verify a finite element numerical model of the joint. From seismic analyses, the SFRC mixes were shown to enhance the seismic performance of the joint compared to plain concrete or traditional reinforced concrete. Due to limited literature information, the main objective of the current research work was to investigate the effect of various types of concretes (with SFRC composite) on the seismic behaviour of the subway tunnel in Tehran. Several models of concrete were also performed to determine the best stiffness of the samples. In addition, we built some samples and experimentally tested them to determine critical parameters. Finally, we examined the effect of compression and tensile strength on the seismic behaviour of samples in terms of displacement and stress.

2 Experimental test

The tests were carried out for the tunnel in the Tehran subway. Excavation and sampling in 36.32 meters depth and the result of the unified classification was three types of soil in this case study. Fig. 1 shows a Flowchart of the Plan, Fig. 2 shows a View of the tunnel in the Tehran subway and in Table 1, the characteristic of soils is presented. The direct cutting test was performed according to ASTM D3080. Also, the dimension of the specimen is $30 \times 30 \times 15$ (cm). Fig. 3 shows a view of the Direct shear machine, and Fig. 4 shows particle size distribution in depth of 0-36.32.

Table 1: Soil characteristics

Soil	**Gradation**			**Att. Limits**		**Classification**	**v**	**C**	φ	**E**
Z(m)	**Fines**	**Sand**	**Gravel**	**LL (%)**	**PI (%)**	**USCS**	$\frac{\mathbf{kn}}{\mathbf{m^2}}$	**{kPa}**	**(degree)**	**kPa**
0-15	32.80	26.62	40.58	33.6	11.1	GC	20	12	38.3	62000
15-18.16	28.77	27.25	43.98	32.4	10.5	GC	20	11	39.4	155000
18.16-36.32	19.28	24.27	56.45	30.3	0.09	GC	20	10	40	105000

The following figures show the test results of the samples based on particles size and stress-strain distribution.

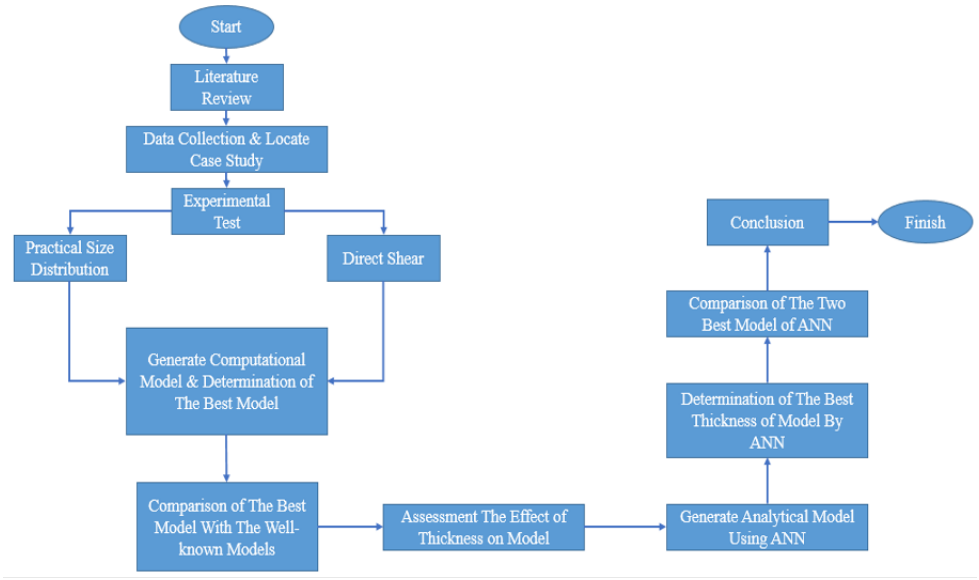

Figure 1: Show the Flowchart of the Plan

Figure 2: View of tunnel in Tehran subway

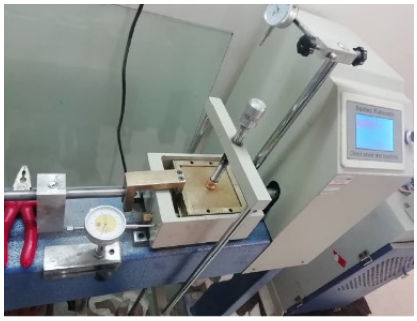

Figure 3: View of the Direct shear machine

3 Modeling

In this paper, the Tehran subway tunnel will be studied. In this research, we use different models of thickness (similar, in terms of compressive strength and tensile strength) that have been evaluated in Tehran Metro and simulate the concretes made in this research for the existing subway in Tehran. Also, for seismic analysis, we use the "Elcentro" earthquake acceleration mapping for numerical modelling. Materials used for soil and concrete modelling are also presented in Table 1.

In this paper, for seismic analysis, the characteristics of the El Centro earthquake that occurred in the United States have been used. The characteristics of this earthquake are shown in Table 2, and its acceleration map is shown in Figure 6. Also, for modelling concrete, one type of concrete model has been used, the specifications of which are presented in Table 3.

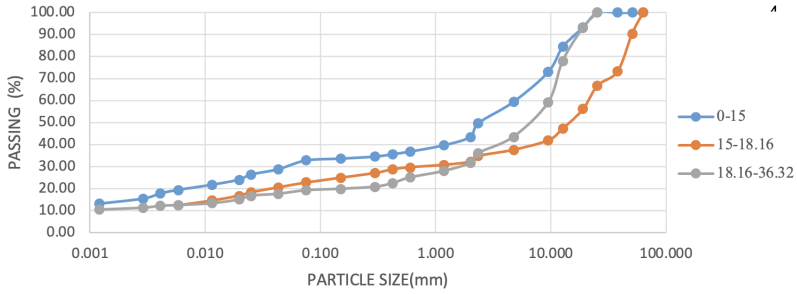

Figure 4: The particle size distribution in depth of 0-36.32

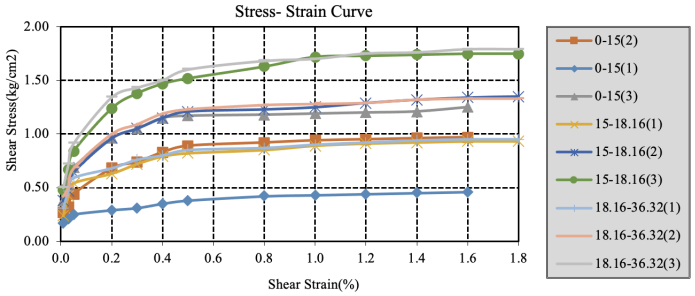

Figure 5: The shear strain- stress in 0-36.32

To accurately simulate the seismic behaviour of the tunnel, we need a preliminary estimate of the dimensions of the computational network cells. Accordingly, finer meshes increase the analysis time as well as the analysis accuracy. But it is not affordable. Larger meshes, on the other hand, drastically reduce the analysis time but also cause severe errors due to successive simplifications. On the other hand, the size of the grid from one value onwards will not affect the solution of the model, and the smaller size only increases the solution time. Hence, we need the analysis of independence in the mesh. To do this, under the same model conditions, we determine the amount of stress and tunnel displacement in different grid sizes. This analysis is presented in Table 4. As can be seen in Table 4, the model with a mesh size of 1.35 has mesh independence, and the mesh is less than that with a difference of half a hundred percent, so the analysis will be done with a mesh size of 1.35. Fig. 7 shows a view of a mesh tunnel model with a mesh size of 1.35.

Table 2: Elcentro Earthquake Specification

Event	Year	Area effect	M_w
Mexico	1941	Mexico and United state	7.2

Table 3: Specifications of concrete used in modeling

MODEL	Macro steel fiber ratio (%)	Micro steel fiber ratio (%)	Compression strength (N/mm2)	Tensile strength (N/mm2)
M4	0.5	0.5	60.8	6.7

Table 4: Mesh independence analysis

Mesh size	Stress ($\frac{n}{m^2}$)	Displacement (cm)	Difference compared to the previous model (%)
1.75	2.531e+06	51.50	-
1.55	2.665e+06	48.14	Stress:5 Displacement: 6.5%
1.35	2.971e+06	52.63	Stress:10% Displacement: 8.5%
1.15	2.969e+06	52.93	Stress:0.06% Displacement: 0.5%

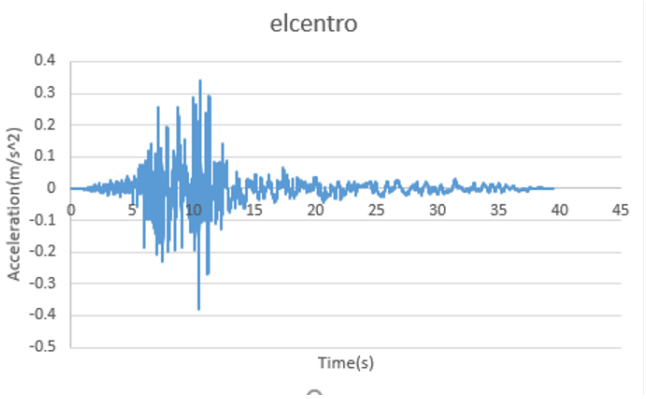

Figure 6: Acceleration map of "Elcentro" earthquake2

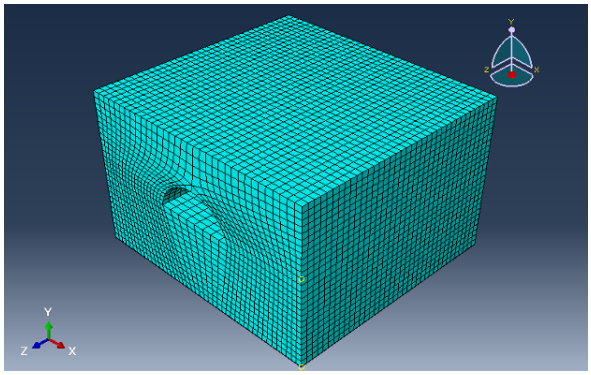

Figure 7: View of the meshed model

4 Results

In this section, the results of the models presented in Table 3 of the metro tunnel under the El Centro record will be presented with the physical properties of SFRC concrete tunnels, all boundary conditions and loading are the same, and only the thickness has changed. Therefore, in Figures 8 and 9, the results related to the analysis and comparison of the models from the point of view of displacement and von Mises stress are presented, respectively.

Also, in order to examine more closely all 3 models (3 models from the SFRC concrete), the results obtained from all 3 designed models to compared easily from the point of view of stress and displacement in Figs., respectively.

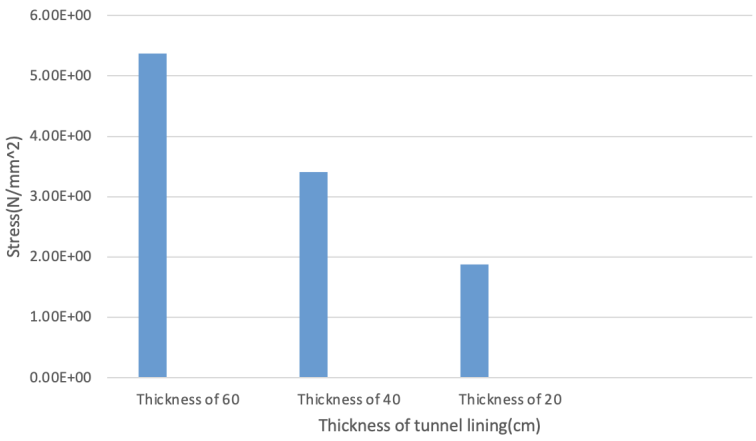

Figure 8: Comparison of the highest stresses in the Elcentro earthquake in 3D analyses

In the table below, a comparison has been made to determine specification from avanaki [2] paper data shows the

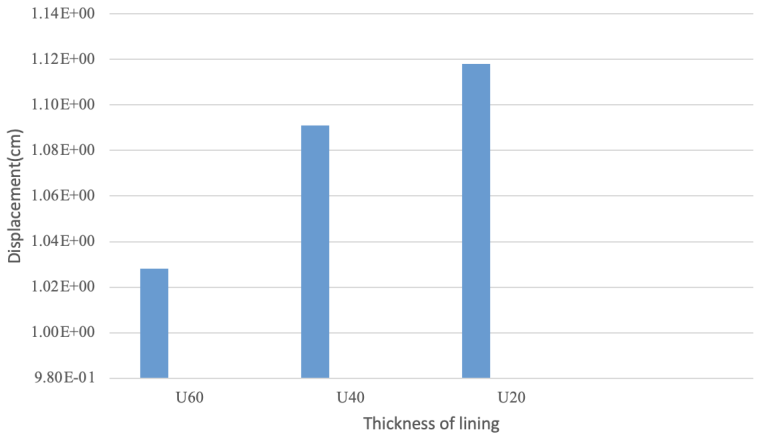

Figure 9: Comparison of the highest displacement in the Elcentro earthquake in 3D analyses

rate of improvement due to the injection of fiber(SFRC) into reinforced concrete (M4) in order to increase the strength of the subway tunnel.

Table 5: Comparison of improvement of model than reinforced concrete

MODEL	Macro steel fiber ratio (%)	Micro steel fiber ratio (%)	Compression strength (N/mm2)	Tensile strength (N/mm2)	Results of Stress (%)	Results of Displacement (%)
M4	0.5	0.5	60.8	6.7	+28	-7.1

In the following, the effect of thickness on the amount of stress and displacement of the tunnel under the El Centro earthquake is investigated. For this purpose, three thicknesses of 20, 40 and 60 cm have been used. Figures 8 and 9 show the effect of thickness on tunnel stress and displacement, respectively. It should be noted that in this case, all border and abutment conditions are considered the same and only the thickness of the tunnel has changed. The result shows that the lowest displacement (1.028 cm) and highest stress (5.371e+06 $\frac{N}{mm^2}$) are to the 60 cm thickness of the tunnel, and the highest displacement(1.18E+00) and lowest stress(1.878E+06) applied to the model with 20 cm thickness.

5 Optimization

According to the study on the effect of thickness on the stress and displacement of the tunnel, the data obtained from the previous step are used for optimization. In other words, in the previous stage and over time, by considering three different thicknesses of 20, 40 and 60 cm of the tunnel, the amount of displacement and stress on the tunnel in each time step has been obtained. At this stage, using coding in MATLAB software, and using two widely used methods of the neural network, namely MLP and RBF neural network, try to find the optimal thickness to reduce stress and displacement for the tunnel under the El Centro earthquake record. In other words, in these two models, there are four input variables, time, thickness of 20 cm, thickness of 40 cm and thickness of 60 cm, which result in two outputs of displacement (meters) and stress (N/mm^2). With these interpretations, we examine and evaluate the network of neural models.

An important topic in neural networks is the trainer function. Table 6 provides a comparison between the regression of different trainer functions to determine which function had the highest performance. It should be noted that in neural network training, data are randomly selected based on a ratio of 30-70, which is a random change in the correlation of the training function. Therefore, the results presented in the table below are the best results among 20 times of performing each training function with 10 layers and 20 neurons.

As can be seen in Table 6, the Levenberg-Marquardt function, known in the MATLAB library as “trainlm”, has the highest correlation value. Hence, this function is used to train the data.

Before modelling MLP and RBF neural networks, it is first necessary to determine the optimal architecture of these models. In the MLP network, the values of the number of layers and the number of neurons, and in the RBF neural network, the values of radial bias or SPREAD, the number of neurons, and the number of neurons in between display

Table 6: Comparison of correlation (regression) of different trainer functions of neural network

row	Trainer Function	Description	Correlation
1	trainlm	Levenberg-Marquardt	0.83096
2	trainscg	Scaled conjugate gradient	0.79822
3	trainbr	Bayesian regularization	0.81745
4	trainbfg	BFGS quasi-Newton	0.71326
5	traincgb	Conjugate gradient backpropagation with Powell-Beale restarts	0.66384
6	traincgp	Conjugate gradient backpropagation with Polak-Ribiére updates	0.79795
7	traingda	Gradient descent with adaptive learning rate	0.78245
8	traingdm	Gradient descent with momentum	0.74142
9	traingdx	Gradient descent with momentum and adaptive learning rate	0.81245
10	trainoss	One-step secant	0.67104

(DF) are the factors affecting the optimal performance of these networks. Based on the various architectures studied, it is found that in the MLP neural network, changing the number of layers from 10 up and down as the number of neurons increases improves performance and increases correlation between data. Therefore, it can be concluded that the best architecture for an MLP neural network is to determine the effect of thickness on stress and displacement equal to 20 layers and 10 neurons. Also, the best architecture for the RBF neural network is SPREAD equal to 1, number of neurons equal to 30, and DF equal to 25. Therefore, having these architectures, we model the effect of thickness parameters on displacement and stress in the tunnel.

The following figure shows the proposed architecture for a neural network with three different thicknesses that ultimately lead to an output (stress or displacement).

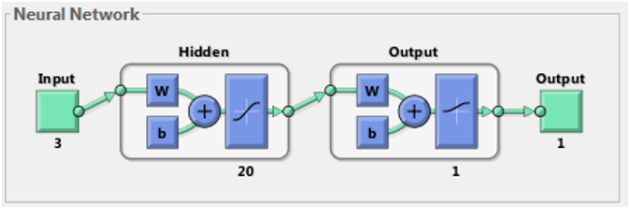

Figure 10: Proposed architecture of MLP

Figures 11 and 12 show the regression estimation diagrams for stress and displacement in the tunnel based on the change in thickness, respectively.

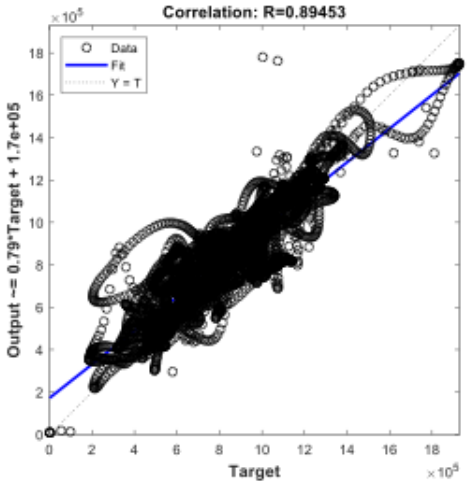

Figure 11: MLP neural network correlation diagram for estimating tunnel stress

Figures 13 and 14 also show the correlation diagrams of stress and displacement performance using RBF neural network architecture, respectively.

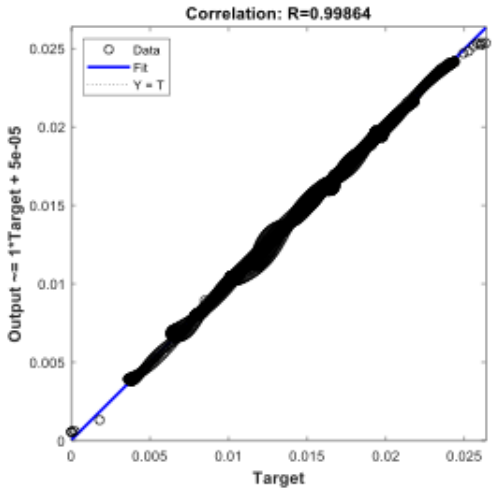

Figure 12: MLP neural network correlation diagram for estimating tunnel displacement

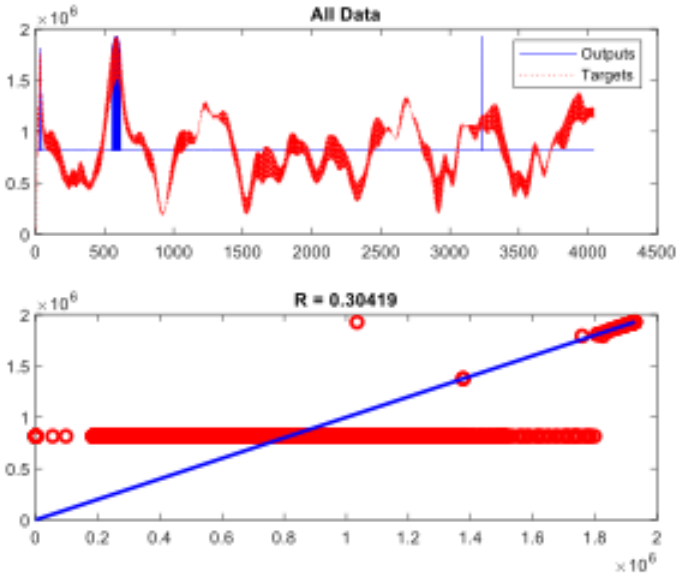

Figure 13: RBF neural network correlation diagram for estimating tunnel stress

According to the modelling, it was found that, firstly, due to the excessive scattering of stress effects on the tunnel, the RBF neural network could not provide the desired results to determine the effect of thickness on the stress on the tunnel. It was also observed that the MLP neural network presented better results than the RBF neural network. Table 7 examines the error and correlation obtained from both neural models for both stress and displacement parameters.

Table 7: Evaluation of MSE error and correlation of MLP and RBF

Models	Displacement		Stress	
	Correlation	MSE	Correlation	MSE
MLP	0.99864	7.0322×10^{-19}	0.89453	0.1484
RBF	0.95908	2.04103×10^{-6}	0.30419	8.367×10^{-8}

Also in Table 8, the optimal thickness of the tunnel for high bearing in the first 3 seconds of applying the earthquake, in which the greatest amount of stress and displacement occurred, using MLP and RBF neural networks to determine the most ideal state between stress and displacement.

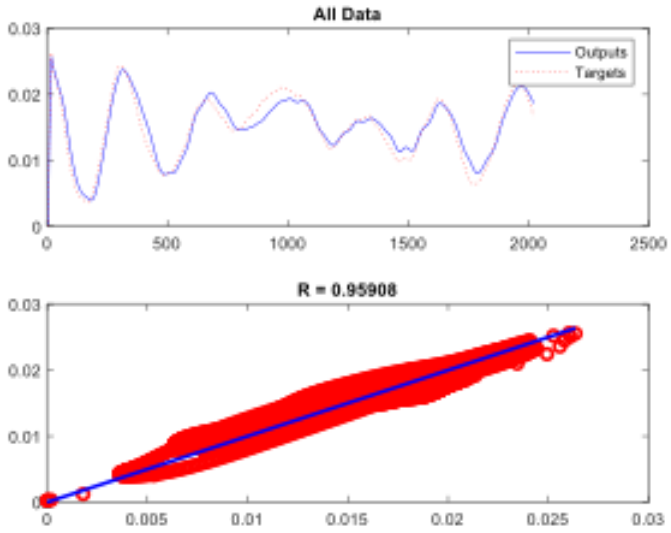

Figure 14: RBF neural network correlation diagram for estimating tunnel displacement

Table 8: Optimal tunnel thickness using MLP and RBF neural networks

Models	Optimum Thichness for Displacement (cm)	Optimum Thichness for Stress (cm)
MLP	47.21	47.95
RBF	48.15	48.22

According to Table 8 and based on the fact that the MLP neural network has a better performance than RBF, it can be concluded that the optimal thickness for the tunnel to control stress is 47.95 cm and to control displacement is 47.21 Cm. This thickness can provide the optimal performance in the most ideal state between stress and displacement at the maximum force applied to the tunnel in the first 3 seconds.

6 Conclusion

In this paper, we model the seismic behaviour of a reinforced tunnel (Tehran Subway) and examine the results of 3 different models of concrete structural materials from the point of view of stress and displacement based on "Elcentro" earthquake records. Comparing the displacement created in all 3 models that differed from each other in the physical properties of concrete, it was found that the highest displacement of 1.118 cm is related to concrete M4(with 60 cm tunnel lining). Based on this, it can be concluded that the model designed by 60 cm lining is the best model i.e. the compression strength is 60.8 N/mm2 and the tensile strength is 6.7 N/mm2). Also, to determine the optimal tunnel thickness, MLP and RBF neural network models were used. The results showed that the MLP network with an MSE error of 0.1937 in determining the stress, and 6.33×10^{-19} had better performance in displacement than the RBF model. It was also found that the optimal thickness of the tunnel using the MLP network to control stress equal to 47.95 cm and to control displacement equal to 47.21 cm, and the RBF network to control stress equal to 48.22 cm and to control displacement equal to 48.15 cm is obtained. Also, it was shown that the maximum stress tolerance by MLP and RBF methods is equal to $1.7556 \times 10^{+6}\ N/m^2$ and $1.9289 \times 10^{+6}\ N/m^2$. And, the highest amount of displacement with both methods was equal to 0.0256 cm.

References

[1] A. Amorosi and D. Boldini, *Numerical modeling of the transverse dynamic behavior of circular tunnels in clayey soils*, Soil Dyn. Earthquake Engin. **29** (2009), no. 6, 1059–1072.

[2] M.J. Avanaki, A. Hoseini, S. Vahdani, and A. De La Fuente, *Numerical-aided design of fiber reinforced concrete tunnel segment joints subjected to seismic loads*, Const. Build. Mater. **170** (2018), no. 12, 40–54.

[3] A. Bobet, *Effect of pore water pressure on tunnel support during static and seismic loading*, Tunnel. Underground Space Technol. **18** (2003), no. 4, 377–393.

[4] H. Huo, A. Bobet, G. Fernández, and J. Ramírez, *Analytical solution for deep rectangular structures subjected to far-field shear stresses*, Tunnel. Underground Space Technol. **21** (2006), no. 6, 613–625.

[5] R.N. Hwang and J. Lysmer, *Response of buried structures to traveling waves*, J. Geotech. Engin. Div. **107** (1981), no. 2, 183–200.

[6] S.E. Kattis, D.E. Beskos, and A.H. D. Cheng, *2D dynamic response of unlined and lined tunnels in poroelastic soil to harmonic body waves*, Earthquake Engin. Struct. Dyn. **32** (2003), no. 1, 97–110.

[7] L.B. Liu, Y. Wang, F. Liu, and J. Zhou, *Shaking table model tests on the influence of fault strike on the seismic responses of tunnels*, J. Vib. Shock **36** (2017), no. 21, 196–202.

[8] X. Liu, B. Guo, X. Li, and Y. Sang, *Model experiment study on effect of deformation joints on road tunnel resisting destruction by thrust fault stick-slip dislocation*, Thrust Fault J. **8** (2015), no. 4.

[9] Y. Liu and F. Gao, *Experimental study on the dynamic characteristics of a tunnel-crossing fault using a shake-table test*, J. Vib. Shock **35** (2016), no. 12, 160–165.

[10] D. Park, M. Sagong, D.Y. Kwak, and C.G. Jeong, *Simulation of tunnel response under spatially varying ground motion*, Soil Dyn. Earthquake Engin. **29** (2009), no. 11, 1417–1424.

[11] J. Penzien, *Seismically induced raking of tunnel linings*, Earthquake Engin. Struct. Dyn. **29** (2000), no. 5, 683–691.

[12] J. Penzien and C.L. Wu, *Stresses in linings of bored tunnels*, Earthquake Engin. Struct. Dyn. **27** (1998), no. 3, 283–300.

[13] M. Russo, G. Germani, and W. Amberg, *Construction of large tunnel through active faults: A recent application*, Int. Conf. Tunnel. Underground Space Use, 2002, pp. 16–18.

[14] D. Wang, G. Cui, and J. Yuan, *Model experimental study on effect of reducing dislocation measures undering stick-slip fault dislocation of tunnel*, Chin. J. Geotech. Engin. **40** (2018), no. 8, 1515-1521.

[15] W. Xiong, W. Fang, and J.B. Peng, *Numerical analysis of effect of normal fault activity on road mountain tunnel project*, Chinese J. Rock Mech. Engin. **29** (2010), no. 1, 2845–2852.

[16] H.T. Yu, J.T. Chen, A. Bobet, and Y. Yuan, *Damage observation and assessment of the Longxi tunnel during the Wenchuan earthquake*, Tunnel. Underground Space Technol. **54** (2016), no. 2, 102–116.

[17] H.T. Yu, J.T. Chen, Y. Yuan, and X. Zhao, *Seismic damage in mountain tunnels due to the Wenchuan strong earthquake*, J. Mountain Sci. **13** (2016), no. 11, 1958–1972.

[18] H.T. Yu, Y. Yuan, X. Liu, Y.W. Li, and S.W. Ji, *Damages of the Shaohuoping road tunnel near the epicentre*, Struct. Infrast. Engin. **9** (2013), no. 9, 935–951.

[19] H.T. Yu, Y. Yuan, G.P. Xu, Q.K. Su, X. Yan, and C. Li, *Multi-point shaking table test for long tunnels subjected to non-uniform seismic loadings - Part II: application to the HZM immersed tunnel*, Soil Dyn. Earthquake Engin. **108** (2018), no. 8, 187–195.

[20] Y. Yuan, H.T. Yu, C. Li, X. Yan, and J.Y. Yuan, *Multi-point shaking table test for long tunnels subjected to non-uniform seismic loadings - Part I: Theory and validation*, Soil Dyn. Earthquake Engin. **108** (2018), no. 8, 177–186.